

Second order dispersion by optimised rotation pulses

David L. Goodwin,^{1,*} Martin R. M. Koos,^{1,2} and Burkhard Luy¹

¹*Institute for Biological Interfaces 4,*

Karlsruhe Institute for Technology (KIT), Karlsruhe, Germany

²*Department of Chemistry, Carnegie Mellon University, Pittsburgh, USA*

(Dated: March 14, 2022)

Abstract

Optimal control has become a useful tool in designing pulses for complicated control problems, beyond the limit of classical hard pulses. Building on past research of broadband pulses performing effective unitary propagation (BURBOP), research presented here presents a class of pulse following adiabatic evolution via second order phase dispersion. This class of pulse performs a rotation around an axis on the transverse plane defined by the phase dispersion. Resulting pulses have equivalently lower energy/higher fidelity when compared to BURBOP.

INTRODUCTION

The critically important milestones on the roadmap of quantum technology development are expected to include quantum optimal control [1, 2]. As an application of optimal control theory, this area of science is tasked with taking a quantum system from one state to another with minimal expenditure of time and energy. Already, this modern scientific method has been applied successfully to a wide range of experiments including nuclear magnetic resonance spectroscopy [3–5], error-correction for quantum computing [6], electron paramagnetic resonance spectroscopy [7, 8], controlled excitation of Bose-Einstein condensates [9], state entanglement for quantum information registers [10], high resolution medical imaging satisfying legal irradiation constraints [11], and robust cold-atom interferometry [12]. In addition to experimental applications, optimal control has advanced theoretical studies calculating gates for quantum computing [13–15].

The growing plethora of reported applications of quantum optimal control is twinned with the concurrent development of optimal control algorithms. This development is essential as desired solutions push to the limit of what is physically possible and control problems become computationally arduous. There are a number of different approaches to optimal control, such as Lagrangian methods [16], time optimal control [17], sophisticated gradient-free searches [18], rapidly converging Krylov-Newton methods [19], and more recently optimal control using analytic controls [20].

This communication is concerned primarily with optimal control problems solved numerically with the piecewise-constant control pulse approximation [3]. The trajectory gradient can be calculated and followed with linear convergence [4], super-linear convergence [21], or quadratic convergence [22, 23], to an optimum destination. Extensions of this method include annealing a quantum system to a desired effective Hamiltonian [5], and utilisation of cooperative multi-pulse control [24].

A subset of desired control targets can be used to construct quantum gates [13–15], being unitary propagators of the system [6], from *universal rotations* [10, 25]. Pulses designed for these applications induce an effective rotation of the coordinate system, with a defined rotation axis and rotation angle, for arbitrary initial state vectors. The development reported in this communication will be concerned with to this class of control pulses.

One of the problems associated with universal rotation solutions is the resulting high

irradiation energy compared with the easier control problem of optimising state-to-state problems [25]. A novel method is presented here which will show this energy can be lowered by defining target propagators as a function of phase dispersion. A customised version of the *Spinach* [26] optimal control toolbox [21, 23, 27, 28] is used to simulate an ensemble of two-level quantum systems and produce these low energy pulses. This class of pulses is named SORDOR (Second ORder Dispersion by Optimised Rotation) pulses by the authors.

BROADBAND OPTIMAL CONTROL TO EFFECTIVE PROPAGATORS

An ensemble of uncoupled two-level systems should include frequency dispersion terms from local environmental conditions, making uniform manipulation of the ensemble a difficult practical task. Although irradiation pulse shapes can be calculated analytically to be robust over a desired bandwidth [29, 30], the ensemble can also be described by a bilinear control problem. The controllable part of the Hamiltonian is the irradiated pulses, and the uncontrollable part is a local frequency dispersion term. Restricting irradiated controls to phase modulation, $\varphi(t)$, the time-dependent Hamiltonian for this ensemble of K uncoupled two-level systems can be written as

$$\hat{H}(t) = \sum_{k=1}^K \omega_k \hat{\sigma}_z^{(k)} + A \cos(\varphi(t)) \hat{\sigma}_x^{(k)} + A \sin(\varphi(t)) \hat{\sigma}_y^{(k)} \quad (1)$$

where ω_k is variously termed resonant frequency offset, chemical shift, or detuning, and describes the local frequency dispersion within the ensemble. $\hat{\sigma}_{x,y,z}^{(k)}$ are operators of the k^{th} two-level system, operating in a Hilbert space, and related to the Pauli matrices $\hat{\sigma}_{x,y,z}$ by

$$\hat{\sigma}_{x,y,z}^{(k)} = E \otimes \hat{\sigma}_{x,y,z} \quad (2)$$

where E is a $K \times K$ matrix of zeros except with $E_{kk} = 1$, and ω_k form a grid of resonance offsets spread over a bandwidth [3, 31].

The GRAPE method of optimal control [4] proceeds to describe the time-dependent irradiation as piecewise constant over a small time interval Δt [3]. This approximation allows numerical solution of Eq. (1) through time-ordered propagation,

$$\begin{aligned} \hat{P}_n &= \exp \left[-i \hat{L}_n \Delta t \right], & \mathcal{U}_n &= \hat{P}_n \dots \hat{P}_2 \hat{P}_1 \\ \mathcal{V}_n &= \hat{P}_{n+1}^\dagger \dots \hat{P}_N^\dagger \mathcal{R} \end{aligned} \quad (3)$$

with the Liouvillian, $\hat{\hat{L}}_n$, an adjoint representation of a Hamiltonian: $\hat{\hat{L}} = \mathbb{1} \otimes \hat{H} - \hat{H}^\dagger \otimes \mathbb{1}$ [21]. At a time increment, n , the effective propagator, \mathcal{U}_n , evolves the system forward in time over the interval $[t_1, t_n]$, and the effective propagator of the adjoint control problem, \mathcal{V}_n , evolves backwards from a desired target, \mathcal{R} , over the interval $[T, t_n]$.

The Hilbert-Schmidt inner product of the desired effective propagator, \mathcal{R} , and the effective propagator over the irradiation duration, \mathcal{U}_N , gives a measure to numerically maximise and is termed the fidelity [4, 5, 10, 25]:

$$\max_{\varphi} \{\mathcal{F}\} = \frac{1}{d} \max_{\varphi} \left\{ \text{Re} \langle \mathcal{R} | \mathcal{U}_N \rangle \right\} \quad (4)$$

This fidelity measure, \mathcal{F} , is normalised with the dimension of the Hilbert space, d , to give sensible and predicable bounds $\mathcal{F} \in [-1, +1]$.

The gradient-following GRAPE method of optimal control requires directional propagator derivatives at each time increment in the direction of each control operator. For phase modulated pulses, the gradient vector is constructed from the elements

$$\frac{\partial \mathcal{F}}{\partial \varphi_n} = A^2 \langle \mathcal{V}_n | \left[\cos(\varphi_n) \frac{\partial \hat{\hat{P}}_n}{\partial \hat{\hat{\sigma}}_y} - \sin(\varphi_n) \frac{\partial \hat{\hat{P}}_n}{\partial \hat{\hat{\sigma}}_x} \right] \mathcal{U}_n \rangle \quad (5)$$

The time propagators in Eq. (3) and their directional derivatives in Eq. (5) can be calculated analytically with one exponentiation of a block-triangular matrix [28, 32],

$$\exp \left[-i \begin{bmatrix} \hat{\hat{L}}_n & \hat{\hat{\sigma}} \\ \mathbf{0} & \hat{\hat{L}}_n \end{bmatrix} \Delta t \right] = \begin{bmatrix} \hat{\hat{P}}_n & \frac{\partial \hat{\hat{P}}_n}{\partial \hat{\hat{\sigma}}} \\ \mathbf{0} & \hat{\hat{P}}_n \end{bmatrix} \quad (6)$$

in each direction $\hat{\hat{\sigma}} \in \{\hat{\hat{\sigma}}_x, \hat{\hat{\sigma}}_y\}$.

ROTATION AXES WITH QUADRATIC PHASE DISPERSION

The ensemble of Eq. (1) can be controlled with adiabatic evolution [33–35], described as a linear frequency sweep over the two-level systems, or equivalently pulses with quadratic phase dispersion. This phase dispersion can be used to define targets of an optimal control method, previously optimised as a state-to-state problem with linear phase dispersion [24, 36–38] and quadratic phase dispersion [29, 33, 39].

Although state-to-state optimal control is useful, it is specific: the control only effective for a defined initial state of the system. A more general control method is to find desired

effective propagators of the two-level system [10, 25] which rotate all components its coordinate system around a defined axis. The axis of rotation can be defined for each member of the ensemble by its phase dispersion

$$\mathcal{R}_k(\beta) = \exp \left[-i \left(\cos(\alpha_k) \hat{\sigma}_x^{(k)} + \sin(\alpha_k) \hat{\sigma}_y^{(k)} \right) \beta \right] \quad (7)$$

where β is the rotation angle, and α_k is the desired phase of the ensemble member. For adiabatic evolution the desired phase dispersion can be derived from Landau-Zener-Stückelberg-Majorana theory [40, 41], given here with quadratic phase dispersion

$$\alpha_k = \frac{\pi QT}{\Omega} \left(-\omega_k^2 \sin^2 \left(\frac{\beta}{2} \right) + \Omega \omega_k \sin(\beta) + \left(\frac{\Omega}{2} \right)^2 \right) \quad (8)$$

where T is the total duration of the pulse, Q is an adiabaticity factor [42] to produce phase dispersed pulses, and Ω is the required bandwidth.

CHAINED OPTIMAL CONTROL

The process of finding the desired optimal solutions set out in EQ. (7) is not trivial. Finding the maximum fidelity in EQ. (4) for K uncoupled two-level systems is equivalent to the arithmetic average of K optimisations, each for a single two-level system in EQ. (1). The standard procedure of starting the optimisation from a random guess, or even from an appropriate adiabatic passage pulse, results in a fidelity profile over the bandwidth with periodically reducing to zero fidelity. As the optimisation continues these sections of zero fidelity become engraved into the fidelity profile – fidelity sections either side of the zeroed fidelity increase, also increasing the average fidelity, trapping this fidelity minima into the problem. This can be viewed as *missed turns* over the offset profile.

A stabilising *unwinding penalty*, penalising parts of the ensemble beyond the *missed turns*, can be designed with a deadzone-quadratic penalty method [23], so unwinding the fidelity beyond the missed turns

$$\mathcal{K} = \frac{1}{K} \left(\|\vec{\mathcal{F}} - g_1\|^2 h_1 + \|\vec{\mathcal{F}} - g_2\|^2 h_2 \right) \quad (9)$$

$$\nabla \mathcal{K} = \frac{2}{K} \left((\vec{\mathcal{F}} - g_1) h_1 + (\vec{\mathcal{F}} - g_2) h_2 \right) \quad (10)$$

where $\vec{\mathcal{F}}$ is the vector representation of the fidelity profile, and $h_{1,2}$ are Heaviside functions

$$h_1 = \begin{cases} 1, & \text{if } \mathcal{F}_k > g_1 \\ 0, & \text{otherwise} \end{cases}, \quad h_2 = \begin{cases} 1, & \text{if } \mathcal{F}_k < g_2 \\ 0, & \text{otherwise} \end{cases} \quad (11)$$

g_1 and g_2 define the bounds of the penalty and are found by inspection of $\mathcal{F}(\alpha_k)$ as the first offset points to have $\mathcal{F}(\alpha_k) = \mathcal{F}_k \approx 0$ either side of zero offset. However, this method becomes unstable and will fail with many missed turns, which should be expected for all but the shortest duration pulses.

This communication sets out a procedure of *chained optimal control* to stabilise the problem of missed turns outlined above:

1. Start with an initial pulse shape of the appropriate BURBOP.
2. Set $j = 0$ and run the *chained optimal control* forward, gradually increasing Q .
 - (a) Run GRAPE optimisation with $Q = j\varepsilon$ near to convergence, stopping when $\|\nabla\mathcal{F}\| \leq \tau$.
 - (b) **If** $\mathcal{K} > 0$ from EQ. (9) at the end of the optimisation, continue to 3 below.
 - (c) **Else**, set the new initial pulse shape from 2a, increment $j = j + 1$, and return to 2a.
3. Run the *chained optimal control* backwards, gradually decreasing Q .
 - (a) **While** $j \geq 0$, run GRAPE optimisation with $Q = j\varepsilon$ near to convergence, stopping when $\|\nabla\mathcal{F}\| \leq \tau$.
 - (b) Set the new initial pulse shape from 3a, decrement $j = j - 1$, and return to 3a.

The authors find it adequate to use $\tau = 10^{-4}$ and $\varepsilon = 0.01$ in the results that follow.

RESULTS

A single spin- $1/2$ ^{13}C nucleus in a static magnetic field of $B_0 = 14.0954$ T is used as the two-level system in EQ. (1). A linearly spaced resonance offset profile, over a bandwidth of 40 kHz, is defined with relation to the pulse duration with $K = 1 + \lceil 4T \times 10^5 \rceil$, representing the uncoupled ^{13}C nuclei.

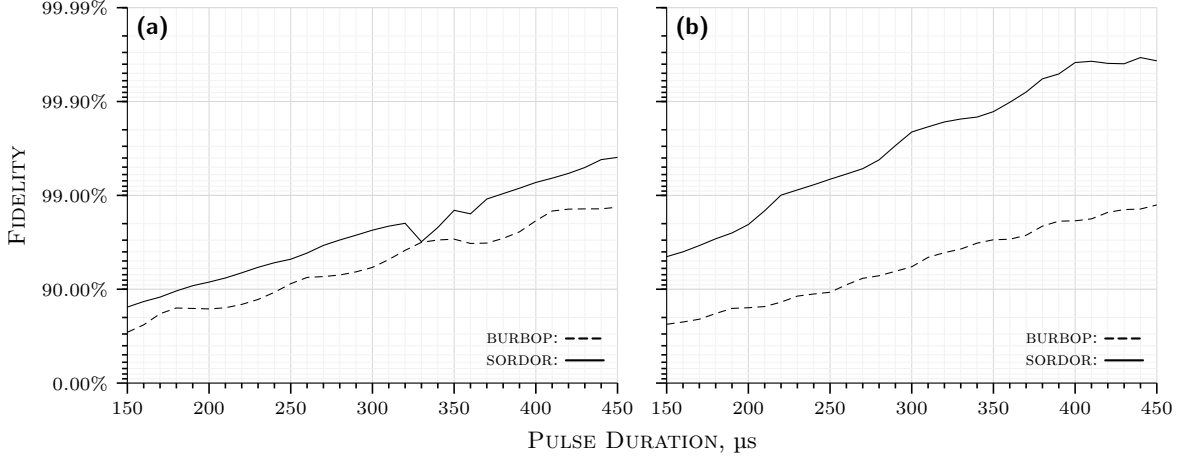


FIG. 1. Comparison of the maximum fidelity achieved for SORDOR and BURBOP, shown for (a) $\beta = \pi/2$ and (b) $\beta = \pi$ rotation angles.

The *Spinach* spin dynamics software toolbox [26] is chosen for the optimal control simulations, with minimal modification to enable optimisation to the desired unitary propagators in EQ. (7), using the ℓ -BFGS(20) optimisation method [21].

A time increment of $\Delta t = 0.5 \mu\text{s}$ with a constant pulse amplitude of $A = 10 \text{ kHz}$ sets the constraints of the phase modulated pulse shapes. The chained optimal control method outlined above is performed for durations $T = 150 \mu\text{s}$ to $450 \mu\text{s}$ in increments of $10 \mu\text{s}$, and for the rotation angles $\beta = \pi/2$ and $\beta = \pi$.

FIG. 1 shows the maximum fidelity achieved in these simulations compared to the fidelity of an equivalent BURBOP pulse. The few points that did not achieve a fidelity according to the visible trend are expected to be improved with further forward and backward chained optimisations (the final shape after the backward chain is not the same as the initial BURBOP pulse), or with a smaller τ . It is the general case that $Q > 0.65$ starts to exhibit the missed turns of EQ. (9).

Particularly for $\beta = \pi/2$, the backward chained optimisation becomes essential in finding the maximum fidelity. Furthermore, the $\beta = \pi/2$ optimisations are much more difficult compared to the $\beta = \pi$ case, and these optimisations take more than twice than amount of computational effort. This should be expected as the $\beta = \pi/2$ case is below the adiabatic threshold, whereas the $\beta = \pi$ case is above the adiabatic threshold [39].

CONCLUSIONS

Optimised pulses giving an effective unitary propagator defining a rotation axis on the transverse plane, with a second order phase dispersion function, can be designed with a combination of chained GRAPE optimisations and an unwinding penalty. Compared to the BURBOP pulses, the SORDOR pulses designed in this communication produce equivalently higher fidelity or lower energy pulses. The trend of this comparison shows $\beta = \pi/2$ SORDOR pulses are approximately 125 μs shorter than BURBOP pulses, and $\beta = \pi$ SORDOR pulses are approximately half of the BURBOP pulses duration. The $\beta = \pi/2$ SORDOR optimisations are the considerably more difficult than $\beta = \pi$ SORDOR optimisations, and although not shown here, a $\beta = \pi$ SORDOR pulse can be similarly designed with the first half of the pulse being the corresponding $\beta = \pi/2$ SORDOR – mimicking the idea of adiabatic half-passage/full-passage pulses.

The difficulty in producing rotation pulses with second phase dispersion, similar to adiabatic passage pulses, is an interesting question on the limits of what pulses can do. Further than this, investigation of the achievable fidelity for a given second order phase dispersion factor defines a class of pulse with the universality of rotation pulses and evolution character of adiabatic pulses.

The methods set out in this communication can also be used to design pulses similar SORDOR, with other phase dispersion functions e.g. of arbitrary or higher order. These methods used to produce phase-modulated SORDOR pulses may also be used to produce phase and amplitude modulated pulses, with care taken to ensure pulse amplitudes stay constrained within defined bounds, and can be calibrated for hardware specific resonator effects [8].

The authors are grateful to Jens Haller, Herbert Ullrich, Michael Garwood, and Malcolm Levitt for insightful comments and discussion. Thanks is given to Ilya Kuprov and Mohammadali Foroozandeh for help finalising this manuscript.

* david.goodwin@kit.edu

[1] S. J. Glaser, U. Boscain, T. Calarco, C. P. Koch, W. Köckenberger, R. Kosloff, I. Kuprov, B. Luy, S. Schirmer, T. Schulte-Herbrüggen, D. Sugny, and F. K. Wilhelm, Eur. Phys. J. D

- 69**, 279 (2015).
- [2] A. Acín, I. Bloch, H. Buhrman, T. Calarco, C. Eichler, J. Eisert, D. Esteve, N. Gisin, S. J. Glaser, F. Jelezko, S. Kuhr, M. Lewenstein, M. F. Riedel, P. O. Schmidt, R. Thew, A. Wallraff, I. Walmsley, and F. K. Wilhelm, *New J. Phys.* **20**, 080201 (2018).
 - [3] T. E. Skinner, T. O. Reiss, B. Luy, N. Khaneja, and S. J. Glaser, *J. Magn. Reson.* **163**, 8 (2003).
 - [4] N. Khaneja, T. Reiss, C. Kehlet, T. Schulte-Herbrüggen, and S. J. Glaser, *J. Magn. Reson.* **172**, 296 (2005).
 - [5] Z. Tošner, S. J. Glaser, N. Khaneja, and N. C. Nielsen, *J. Chem. Phys.* **125**, 184502 (2006).
 - [6] J. Zhang, R. Laflamme, and D. Suter, *Phys. Rev. Lett.* **109**, 100503 (2012).
 - [7] P. E. Spindler, Y. Zhang, B. Endeward, N. Gershernzon, T. E. Skinner, S. J. Glaser, and T. F. Prisner, *J. Magn. Reson.* **218**, 49 (2012).
 - [8] D. L. Goodwin, W. K. Myers, C. R. Timmel, and I. Kuprov, *J. Magn. Reson.* **297**, 9 (2018).
 - [9] R. Bücker, T. Berrada, S. van Frank, J.-F. Schaff, T. Schumm, J. Schmiedmayer, G. Jäger, J. Grond, and U. Hohenester, *J. Phys. B* **46**, 104012 (2013).
 - [10] F. Dolde, V. Bergholm, Y. Wang, I. Jakobi, B. Naydenov, S. Pezzagna, J. Meijer, F. Jelezko, P. Neumann, T. Schulte-Herbrüggen, J. Biamonte, and J. Wrachtrup, *Nat. Commun.* **5**, 3371 (2014).
 - [11] M. S. Vinding, D. Brenner, D. H. Y. Tse, S. Vellmer, T. Vosegaard, D. Suter, T. Stcker, and I. I. Maximov, *Magn. Reson. Mater. Phys.* **30**, 29 (2017).
 - [12] J. C. Saywell, I. Kuprov, D. Goodwin, M. Carey, and T. Freegarde, *Phys. Rev. A* **98**, 023625 (2018).
 - [13] T. Schulte-Herbrüggen, A. Spörl, N. Khaneja, and S. J. Glaser, *Phys. Rev. A* **72**, 042331 (2005).
 - [14] M. Grace, C. Brif, H. Rabitz, I. A. Walmsley, R. L. Kosut, and D. A. Lidar, *J. Phys. B* **40**, S103 (2007).
 - [15] E. Zahedinejad, J. Ghosh, and B. C. Sanders, *Phys. Rev. Lett.* **114**, 200502 (2015).
 - [16] J. Somló, V. A. Kazakov, and D. J. Tannor, *Chem. Phys.* **172**, 85 (1993).
 - [17] N. Khaneja, R. Brockett, and S. J. Glaser, *Phys. Rev. A* **63**, 032308 (2001).
 - [18] P. Doria, T. Calarco, and S. Montangero, *Phys. Rev. Lett.* **106**, 190501 (2011).
 - [19] G. Ciaramella, A. Borzì, G. Dirr, and D. Wachsmuth, *SIAM J. Sci. Comput.* **37**, A319 (2015).

- [20] S. Machnes, E. Assémat, D. Tannor, and F. K. Wilhelm, Phys. Rev. Lett. **120**, 150401 (2018).
- [21] P. de Fouquieres, S. G. Schirmer, S. J. Glaser, and I. Kuprov, J. Magn. Reson. **212**, 412 (2011).
- [22] P. de Fouquieres, Phys. Rev. Lett. **108**, 110504 (2012).
- [23] D. L. Goodwin and I. Kuprov, J. Chem. Phys. **144**, 204107 (2016).
- [24] M. Braun and S. J. Glaser, New J. Phys. **16**, 115002 (2014).
- [25] K. Kobzar, S. Ehni, T. E. Skinner, S. J. Glaser, and B. Luy, J. Magn. Reson. **225**, 142 (2012).
- [26] H. Hogben, M. Krzystyniak, G. Charnock, P. Hore, and I. Kuprov, J. Magn. Reson. **208**, 179 (2011).
- [27] I. Kuprov and C. T. Rodgers, J. Chem. Phys. **131**, 234108 (2009).
- [28] D. L. Goodwin and I. Kuprov, J. Chem. Phys. **143**, 084113 (2015).
- [29] T. E. Skinner and N. I. Gershenson, J. Magn. Reson. **204**, 248 (2010).
- [30] J. S. Li, J. Ruths, and S. J. Glaser, Nat. Commun. **8**, 446 (2017).
- [31] D. Daems, A. Ruschhaupt, D. Sugny, and S. Guérin, Phys. Rev. Lett. **111**, 050404 (2013).
- [32] C. F. Van Loan, IEEE Trans. Automat. Contr. **23**, 395 (1978).
- [33] S. Meister, J. T. Stockburger, R. Schmidt, and J. Ankerhold, J. Phys. A **47**, 495002 (2014).
- [34] Z. Leghtas, A. Sarlette, and P. Rouchon, J. Phys. B **44**, 154017 (2011).
- [35] N. Augier, U. Boscain, and M. Sigalotti, SIAM J. Contr. Optim. **56**, 4045 (2018).
- [36] N. I. Gershenson, T. E. Skinner, B. Brutscher, N. Khaneja, M. Nimbalkar, B. Luy, and S. J. Glaser, J. Magn. Reson. **192**, 235 (2008).
- [37] M. R. M. Koos, H. Feyrer, and B. Luy, Magn. Reson. Chem. **53**, 886 (2015).
- [38] M. R. M. Koos, H. Feyrer, and B. Luy, Magn. Reson. Chem. **55**, 797 (2017).
- [39] C. Brif, M. D. Grace, M. Sarovar, and K. C. Young, New J. Phys. **16**, 065013 (2014).
- [40] L. D. Landau, Phys. Z. Sowjetunion **2**, 46 (1932).
- [41] C. Zener, Proc. R. Soc. London A **137**, 696 (1932).
- [42] J. Baum, R. Tycko, and A. Pines, Phys. Rev. A **32**, 3435 (1985).